



Late time cosmology in $f(R, \mathcal{G})$ gravity with exponential interactions

A. Chanda^{1,a}, A. Halder^{2,b}, A. S. Majumdar^{2,c}, B. C. Paul^{1,d} 

¹ Physics Department, University of North Bengal, Raja Rammohunpur 734013, India

² S. N. Bose National Centre for Basic Sciences, JD Block, Sector III, Salt Lake City, Kolkata 700106, India

Received: 24 October 2022 / Accepted: 5 December 2022 / Published online: 16 January 2023

© The Author(s) 2023, corrected publication 2023

Abstract Cosmological models with $f(R)$ modified gravity are significant to investigate the present and late-time behavior of the Universe. The dynamics of the Universe is studied in the framework of $f(R) = R + \gamma R^2 - \lambda \left(\frac{R}{3m_s^2}\right)^\delta$ gravity (γ, λ, δ are arbitrary constants) with a coupled Gauss–Bonnet (GB) term in the gravitational action and estimate the constraints on the model parameters as well as the late time behavior of the Universe. In this case, the coupled Gauss–Bonnet term is coupled with a free scalar field in the presence of interacting fluid. In addition, we investigate the same for a different form of gravity $f(R) = R$, where the coupled GB term is coupled with a scalar field in a self-interacting potential.

1 Introduction

Modern cosmology has passed through a remarkable transition from speculative science to an experimental one in recent years. This is mostly due to the high precision observations like Supernova Ia, Baryon Acoustic Oscillations (BAO), Cosmic Microwave Background (CMB) measurements etc. [1–6], which have imposed tight constraints on the theoretical models. Cosmological and astronomical observations predict that the present universe is passing through an accelerated phase of expansion. The accelerating nature of the universe along with the issue of dark matter are two of the most challenging problems in modern cosmology. The standard model of cosmology can explain this accelerated phase of expansion of the universe by introducing a cosmological

constant (Λ) [7–10]. The Λ cold dark matter (Λ CDM) model is the most successful model to describe the dark energy (DE) era. Although the model is fairly compatible with the cosmic microwave background data, the existence of both the constituents of the model are in question. Recent observations have further established the fact that the expansion rate of the universe based on local data is different in comparison to the expansion rate which the universe had in the past based on the cosmic microwave background data, an issue known as the Hubble tension [11–15]. The Λ CDM model also suffers from the serious problem of fine tuning [16].

An alternative approach is to modify the geometrical sector of the Einstein field equations (EFE) to fit the missing matter-energy content of the observed universe. Various modified theories of gravity have been considered in the literature [17–26] to describe the evolution of the universe. Such theories can provide a successful description of the late time DE dominated era and can also explain the early inflation [27] with different coupling parameters. A large class of works in modified gravity consider higher order curvature invariants in the Einstein–Hilbert action which leads to curvature based $f(R)$ gravity formalisms [28]. Other modified theories of gravity have also been proposed such as $f(\mathcal{T})$ models [29–31], and $f(\mathcal{G})$ gravity [32], etc. Such modified theories offer several possibilities for theoretical descriptions of cosmology and astrophysics in conformity with observations.

The DE era of the universe has been widely modeled through the $f(R)$ theory of gravity. In $f(R)$ gravity models the modifications to general relativity (GR) appear naturally in the low energy limit of the effective actions [33] of promising candidates of quantum gravity, such as superstring theory. The advantage of $f(R)$ theory of gravity lies in the fact that these models are conformally related to GR with a self-interacting scalar field and can unify both early inflation and the late time acceleration of the universe [34, 35]. In fact,

^a e-mail: anirbanchanda93@gmail.com

^b e-mail: ashadul.halder@gmail.com

^c e-mail: archan@bose.res.in

^d e-mail: bc paul@nbu.ac.in (corresponding author)

the inflationary cosmological scenario was first obtained by Starobinsky [27] in a higher derivative theory of gravity. Cosmological models can be constructed in the $f(R)$ theory of gravity following two different approaches, viz., the Palatini approach where the field equations are second-order differential equations [36–39], and the metric variational approach where the field equations are of fourth order [40]. Different functional forms of $f(R)$ have been considered to study cosmological and astrophysical scenarios [41–48]. Solar system tests are implemented to check the viability of these models [49–54]. However, it may be noted that a cosmological model which fails the solar system test can admit the present accelerating universe. These local tests can thus be bypassed in favor of an independent test at a cosmological scale [55–59].

Recently, a particular class of cosmological models have received attention, where the cosmic fluid components interact with each other via energy exchange [60–64]. Interacting cosmologies are interesting because of their physical as well as mathematical properties. Interactions are introduced in several cosmological scenarios to obtain a complete description of the universe. The cosmic matter sector may possess multiple interacting components as shown in case of M theory, inflationary models and also in case of the accelerating universe [65–70]. The cosmic fluid components violate the energy conservation equation individually, but the total energy density remains conserved. It should be pointed out here that the role of interaction is not to explain the current accelerating phase of the universe, rather, it could provide a plausible solution of the cosmic coincidence problem. In the literature a number of authors have investigated this issue [71–80]. The addition of interaction among the dark components of the universe can also help alleviate the tension on the local Hubble constant [81, 82].

In this work the dynamics of late type evolution of the universe is studied in the framework of $f(R, \mathcal{G})$ gravity with interacting components. We consider an exponential form of interaction to study the effect of the interaction parameter on the dynamics of evolution, as it is the simplest generalization of the usual linear interaction forms [83]. The gravitational action has a Gauss–Bonnet (GB) term coupled to a scalar field. Einstein–Gauss–Bonnet theory can provide a viable description of the dynamics of the early universe as well as the late time era. In the usual four-dimensional framework, the GB terms do not contribute to the dynamics of the universe, however, when coupled with a scalar dilaton field in the gravitational action, they can significantly alter the phenomenology of the universe evolution. (For a detailed review of GB cosmology see Refs. [84–88]). In the present analysis, we investigate the dynamics of an interacting cosmological model of $f(R)$ gravity with a GB term. We further analyze the viability of our model against the backdrop of recent observational data.

The paper is organised as follows: in Sect. 2, we obtain the field equations in $f(R)$ gravity coupled to a GB term. The cosmological parameters to probe the Universe are also obtained. In Sect. 3, we consider interaction among the cosmic fluid components, namely the non-relativistic matter sector which includes dark matter, and the dark energy. The conservation equation is rewritten incorporating the interaction terms. In Sect. 4, we obtain cosmological models in the framework of two different modified theories of gravity and investigate the late time evolution of the universe. In Sect. 5, we probe our model with the observed data of type Ia supernovae (UNION 2.1 data) and obtain the constrain on the model parameters. Finally in Sect. 6 we summarize the results obtained followed by a brief discussion.

2 Background of $f(R)$ -modified gravity with Gauss–Bonnet terms

In this section we describe the basic features of $f(R)$ -modified gravity coupled with the Gauss–Bonnet (GB) terms in presence of a scalar dilaton field. The modified action in this case in $(3 + 1)$ dimensions is given by [89],

$$S = \int d^4x \sqrt{-g} \left(\frac{1}{2\kappa^2} f(R) - \frac{1}{2} g^{\mu\nu} \partial_\mu \phi \partial_\nu \phi - V(\phi) - \xi(\phi) \mathcal{G} + L_m \right), \quad (1)$$

where R denotes the Ricci scalar, $\kappa = \frac{1}{M_P}$ is the gravitational constant with M_P being the reduced Planck mass, $V(\phi)$ is the potential associated with the scalar field, and $\xi(\phi)$ is the Gauss–Bonnet coupling function which depends on the dilaton field. The Gauss–Bonnet invariant is given by $\mathcal{G} = R^2 - 4R_{\mu\nu}R^{\mu\nu} + R_{\mu\nu\sigma\rho}R^{\mu\nu\sigma\rho}$ where $R_{\mu\nu}$ and $R_{\mu\nu\sigma\rho}$ are the Ricci and Riemann curvature tensors respectively. The matter Lagrangian corresponding to both relativistic and non-relativistic perfect fluids is denoted by L_m . The dynamics of evolution of the universe depends significantly on the functional form of the $f(R)$ -modified gravity. To describe the background spacetime geometry we consider a flat Friedmann–Robertson–Walker (FRW) metric in this study. The line element is given by,

$$ds^2 = -dt^2 + a(t)^2 \delta_{ij} dx^i dx^j \quad (2)$$

with $a(t)$ being the scale factor of the universe. For the chosen background geometry, the Ricci scalar and the Gauss–Bonnet invariant can be expressed as, $R = 6(2H^2 + \dot{H})$ and $\mathcal{G} = 24H^2(H^2 + \dot{H})$, where the overdot (“.”) denotes differentiation with respect to cosmic time t and $H = \frac{\dot{a}}{a}$ is the Hubble parameter. The scalar field is assumed to be homogeneous which depends only on the cosmic time.

Variation of the gravitational action with respect to the metric tensor ($g_{\mu\nu}$) and the scalar field (ϕ) leads to the field equations for the gravitational sector as well as the scalar field given by,

$$H^2 = \frac{\kappa^2}{3f_R} \left(\rho + \frac{1}{2}\dot{\phi}^2 + V(\phi) \right) + \frac{f_R R - f}{6f_R} - \frac{H\dot{f}_R}{f_R} + \frac{8\kappa^2 \dot{\xi} H^3}{f_R}, \tag{3}$$

$$\dot{H} = -\frac{\kappa^2}{2f_R} \left(\rho + P + \dot{\phi}^2 \right) - \frac{\ddot{f}_R - H\dot{f}_R}{2f_R} + \frac{8\kappa^2 \dot{\xi} H \dot{H}}{f_R}, \tag{4}$$

$$V_\phi + \ddot{\phi} + 3H\dot{\phi} = \xi_\phi \mathcal{G}, \tag{5}$$

where, ρ and P denote the matter density and pressure of the cosmic fluid respectively and the suffix ϕ represents derivative w.r.t. scalar field ϕ , also $f_R = \frac{\partial f}{\partial R}$. We assume that the cosmic fluid is composed of two different type of fluids, namely non-relativistic matter which is composed of baryons, leptons as well as cold dark matter (CDM) and relativistic matter components which is mainly composed of photons and neutrinos. Therefore the total energy density and pressure of the cosmic fluid are taken as,

$$\rho = \rho_1 + \rho_r \tag{6}$$

$$P = \sum_i \omega_i \rho_i \tag{7}$$

where, $\rho_r = \zeta \rho_2$ and ρ_1, ρ_2 are the energy densities of the fluids, $\zeta = \frac{\rho_{20}}{\rho_0}$ with ρ_{20} being the current density of relativistic matter, ρ_0 is the present value of energy density for non-relativistic matter and ω_i is the equation of state (EoS) parameter for the i th fluid. Though the present energy density for radiation is almost negligible, in order to probe the evolution of the universe for a modest fractional value of the radiation we consider the second term in Eq. (6).

The evolution of the universe can be better visualized in terms of the redshift parameter z which can be measured for different cosmological sources. Thus, to study the late time evolution of the universe we substitute cosmic time t by the redshift parameter (z) with late time universe being represented by low redshifts close to zero. The scale factor of the universe then becomes,

$$a(t) = \frac{1}{1+z} \tag{8}$$

where the present size of the universe (a_0) is assumed to be unity. We also replace the time derivative by the derivative w.r.t. the redshift parameter (z) as,

$$\frac{d}{dt} \equiv -H(1+z) \frac{d}{dz}. \tag{9}$$

Using Eq. (9) all the time derivatives can be replaced by the derivatives with respect to z and we obtain the following relations:

$$\ddot{H} = -H(1+z)H' \tag{10}$$

$$\dot{\phi} = -H(1+z)\phi' \tag{11}$$

$$\ddot{\phi} = H^2(1+z)^2\phi'' + H^2(1+z)\phi' + HH'(1+z)^2\phi' \tag{12}$$

$$\dot{f}_R = \dot{R}f_{RR} + \dot{\phi}f_{R\phi} \tag{13}$$

$$\dot{R} = 6H(1+z)^2(HH'' + (H')^2) - \frac{3HH'}{1+z}. \tag{14}$$

These relations will be used to rewrite the field equations obtained earlier.

We recast the field Eqs. (3) and (5) in the following form,

$$H^2 = \frac{\kappa^2}{3f_R} \left(\rho + \frac{1}{2}\dot{\phi}^2 + V(\phi) \right) + \frac{f_R R - f}{6f_R} - \frac{H\dot{f}_R}{f_R} - \frac{8\kappa^2(1+z)\xi'H^4}{f_R}, \tag{15}$$

$$V_\phi + \ddot{\phi} + 3H\dot{\phi} = \xi_\phi \mathcal{G} \tag{16}$$

where the ‘‘prime’’ ($'$) denotes differentiation with respect to the redshift parameter (z). We have rewritten only two of the three field equations as these two equations will be sufficient to describe the dynamics of the evolution of the late universe. To study the cosmological behaviour of the model we now define a new density parameter as [89–94],

$$\Omega_H = \frac{\rho_{DE}}{\rho_0}, \tag{17}$$

where ρ_{DE} denotes the DE density. The parameter Ω_H will be used to investigate the evolution of the universe and the nature of DE. Instead of using Hubble rate and its derivatives to quantify the cosmological evolution we will use Ω_H to study evolution of the universe. The dark energy density in this case is assumed to be composed of all the geometric terms arising in the Friedmann equation and can be expressed as,

$$\rho_{DE} = \frac{1}{2}\dot{\phi}^2 + V + \frac{f_R R - f}{2\kappa^2} - \frac{3H\dot{f}_R}{\kappa^2} + 24\xi H^3 + \frac{3H^2}{\kappa^2}(1 - f_R). \tag{18}$$

One may reproduce the usual forms of the Friedmann equations of GR using Eqs. (18), (3) and (4) which are given by,

$$H^2 = \frac{\kappa^2}{3} \left(\rho + \rho_{DE} \right) \tag{19}$$

$$\dot{H} = -\frac{\kappa^2}{2} \left(\rho + P + \rho_{DE} + P_{DE} \right) \tag{20}$$

where, P_{DE} represents the pressure corresponding to the dark energy component. The Hubble rate can be expressed

in terms of the density parameter Ω_H as,

$$H^2 = m_s^2 \left[y_H(z) + \frac{\rho}{\rho_0} \right] \tag{21}$$

where, $m_s^2 = \kappa^2 \frac{\rho_0}{3} = 1.87101 \times 10^{-67}$.

Taking the derivatives of the above expression with respect to the redshift parameter (z) we get,

$$HH' = \frac{m_s^2}{2} \left(y_H'(z) + \frac{\rho'}{\rho_0} \right), \tag{22}$$

$$H'^2 + HH'' = \frac{m_s^2}{2} \left(y_H''(z) + \frac{\rho''}{\rho_0} \right), \tag{23}$$

which will be used to formulate the cosmological parameters. To study the late time evolutionary behaviour of the universe one has to solve the field equations (15) and (16). The equations are highly non-linear, so we adopt numerical techniques to solve them with respect to the density parameter Ω_H and scalar field ϕ . The evolutionary behaviour of different cosmological parameters will be plotted here with the redshift (z) for two different models. To differentiate between different DE models quantitatively, a geometrical analysis called statefinder diagnostic was proposed by Sahni et al. [95]. To study the nature of DE we define the equation of state (EoS) parameter ω_{DE} and the density parameter Ω_{DE} with respect to z and Ω_H as [89],

$$\omega_{DE} = -1 + \frac{1+z}{3} \frac{d \ln y_H}{dz} \quad \Omega_{DE} = \frac{y_H}{y_H + \frac{\rho}{\rho_0}}. \tag{24}$$

However for a complete understanding of the cosmological evolution one has to determine the following parameters,

$$q = -1 - \frac{\dot{H}}{H^2}, \quad j = \frac{\ddot{H}}{H^2} - 3q - 2, \tag{25}$$

$$s = \frac{j-1}{3(q-\frac{1}{2})}, \quad Om(z) = \frac{(\frac{H}{H_0})^2 - 1}{(1+z)^3 - 1},$$

where q is the deceleration parameter, j is the jerk parameter, s is the snap parameter and $Om(z)$ is the Om parameter. In this work we consider an interacting cosmic fluid model where the transfer of energy from one sector to another begins at time $t = t_i$, when the interactions originate among the different cosmic fluid components which will be considered in the following section.

3 Conservation equations for interacting fluids

We consider an interacting cosmic fluid scenario where the dark energy interacts with the non-relativistic matter sector. The relativistic particles do not take part in the interactions. The interaction is assumed to originate at a later epoch. Such

interactions may originate due to a variety of mechanisms during particular eras. In case of various scalar field models of DE, such as quintessence or k-essence, phase transitions arise during several cosmological epochs, which result in decay of the cosmological vacuum energy as well as particle production. For the FLRW line element considered above, the conservation equations with interactions can be written as [60–64]:

$$\dot{\rho}_1 + 3H(\rho_1 + P_1) = -Q \tag{26}$$

$$\rho \dot{\rho}_{DE} + 3H(\rho_{DE} + P_{DE}) = Q \tag{27}$$

where, ρ_1 , P_1 and ρ_{DE} , P_{DE} are the energy density and pressure corresponding to the non-relativistic matter and dark energy, respectively. Here Q represents the interaction strength which may assume arbitrary forms. Depending on the sign of Q one can determine the direction of energy flow between the two components. When $Q > 0$, energy flows from the non-relativistic matter sector to the dark energy sector, whereas $Q < 0$ corresponds to the energy loss from the dark energy sector. It is evident from Eqs. (26) and (27) that although the individual fluids violate the conservation equations the total energy density of satisfies the conservation equation together. One can construct an equivalent uncoupled set of energy conservation equations as [96]:

$$\dot{\rho}_1 + 3H(1 + \omega_1^{eff})\rho_1 = 0 \tag{28}$$

$$\rho \dot{\rho}_{DE} + 3H(1 + \omega_{DE}^{eff})\rho_{DE} = 0, \tag{29}$$

i.e.,

$$\sum_{i=1}^3 \left[\rho_i + 3H(1 + \omega_i^{eff})\rho_i \right] = 0, \tag{30}$$

where ω_i^{eff} is the effective equation of state parameter corresponding to the cosmic fluid components. The effective EoS parameters are given by:

$$\omega_1^{eff} = \omega_1 + \frac{Q}{3H\rho_1} \tag{31}$$

$$\omega_{DE}^{eff} = \omega_{DE} - \frac{Q}{3H\rho_{DE}}. \tag{32}$$

The forms of these interactions are not constrained to specific functions. Certain phenomenological choices are initially made and later they are tested using observational data. In the literature several functional forms of interaction rates are considered as, $Q \propto \rho_{DE}$ [97], $Q \propto \rho_1$ [77–80], $Q \propto (\rho_1 + \rho_{DE})$ [77–80], $Q \propto \rho_{DE}^2$ [98], $Q \propto \frac{\rho_{DE}^2}{\rho_1}$ [99], etc. Several of these interaction forms agree with the observational data and lead to stable cosmological models [100, 101]. Thus, any new form of interaction must be constrained using the current observations. In this work we consider an expo-

nential form of interaction as [83]:

$$Q = 3H\eta\rho_{DE} \exp\left(\frac{\rho_{DE}}{\rho_1} - 1\right) \tag{33}$$

where, η is a coupling parameter which denotes the strength of the interaction. We denote the ratio of energy densities of these two fluids as $\alpha = \frac{\rho_{DE}}{\rho_1}$. The above interaction can be rewritten in terms of α as $Q = 3H\eta\rho_{DE}\exp(\alpha - 1)$. Thus, the exponential form of interaction reduces to the linear form when $\alpha \rightarrow 1$ i.e., $Q = 3H\eta\rho_{DE}$, while for $\alpha \rightarrow 0$, $Q \approx 3H\eta\rho_{DE}$. These limits have been studied earlier in the literature [98]. The Taylor series expansion of Eq. (33) around $\rho_{DE} = 0$ yields,

$$Q \propto \rho_{DE} + \frac{\rho_{DE}^2}{\rho_1} + \dots \tag{34}$$

One can thus study the effects of the higher order terms present in the interaction and compare their effect with the linear counterpart. Recently Yang et al. considered this exponential interaction model and drew a comparison between different interaction scenarios [83]. It is noted that the exponential model exhibits a considerable deviation near the present epoch (i.e., $z = 0$).

One can express the energy densities of the non-relativistic and relativistic matters as:

$$\rho_1 = \rho_0(1+z)^{3(1+w_1^{eff})} \tag{35}$$

$$\rho_2 = \rho_{20}(1+z)^4. \tag{36}$$

One can express the total energy density using Eqs. (35) and (36) as:

$$\rho = \rho_0\left[(1+z)^{3(1+w_1^{eff})} + \zeta(1+z)^4\right]. \tag{37}$$

One can solve field equations (15) and (16) numerically using the expressions for energy densities and the parameters Ω_H , and the scalar field ϕ can be determined. The evolution of the universe can be studied through the behaviour of the state finder parameters, the scalar field ϕ , and other cosmological parameters like the deceleration parameter q , $Om(z)$ parameter, etc. The interaction strength η acts as a free parameter in this case along with the function $f(R)$, potential function $V(\phi)$ and the GB coupling term $\xi(\phi)$. One has to consider specific forms of these functions to study the late time dynamics of the universe in presence of interacting cosmic fluid components. The interaction strength severely affects the evolution of the universe which will be studied in the next section.

4 Cosmological models in the modified $f(R)$ gravity with GB terms in the presence of interacting cosmic fluid

We consider different forms of the coupling function for the GB terms with a scalar field in presence of interacting cosmic fluids to study the dynamics of evolution of the late universe. Two different $f(R)$ gravity models are considered here.

4.1 Model-I

We begin our study by considering the simple Einstein gravity (i.e. $f(R) = R$) with Gauss–Bonnet terms coupled to a scalar field. In recent years there is a spurt in activities to search for a viable universe in the framework of modified theories of gravity that emerged as an alternative for dark energy in order to accommodate the present accelerating phase of the universe satisfactorily. A number of modified theories of gravity came up in the literature to study the early and late evolutionary phases of the universe which however finally unify them within a single theoretical framework [111–116].

The string-inspired modified theories of gravity are one of the promising candidates. Zweibach first pointed out that the string corrections due to the Einstein action up to first order in the slope parameter and fourth power of the momenta should be proportional to the GB terms and leads to a ghost-free non-trivial interacting theory [117]. Later it was shown that the field redefinition theorem of Hooft and Veltman [118,119] may apply in this case. Thus the GB terms arise in the low-energy effective action for the heterotic strings [120–123] and also in the second order terms in the Lovelock gravity [124]. It is known that the GB term in 4 dimensions is a constant which does not play any role in explaining the dynamics of the universe. However, the scalar field coupled with the GB terms is important and a number of features of the universe can be explored. A non-singular universe can be obtained in a string-induced gravity with GB term near the initial singularity [125,126]. The string-inspired scalar Gauss–Bonnet gravity as well as the modified GB gravity have been employed to investigate the gravitational dark energy [127].

Recently, scalar GB and modified GB theories have been reconstructed for a given expansion of the universe with and without matter [128]. The bouncing cosmological scenario is investigated in the framework of scalar GB gravity in both the Jordan (string) frame and the Einstein frame [129]. Cosmological solutions of the field equations obtained from a ten-dimensional action differing from the superstring corrected action and containing higher derivative terms in the GB combination have been studied by Paul and Mukherjee [130]. They found realistic cosmological scenarios in presence of an inflationary era in the early ten-dimensional universe. The emergent universe scenario has also been investigated in the framework of scalar GB gravity [131,132]. The

role of scalar coupled GB terms in the dynamics of evolution of the late universe has been investigated considering a three-component cosmic fluid [89]. The scalar coupling function $\xi(\phi)$ is constrained considering the primordial gravitational wave speed.

In the present paper we introduce a non-linear coupling between the cosmic fluid components in order to study the role of interaction between the fluid components. The scalar potential is assumed to be coupled with the dilaton field in this case. The functional form of the scalar field potential is assumed to be:

$$V(\phi) = \left(\frac{\phi}{M_P} \right)^4 \quad (38)$$

with a scalar coupling function of the form,

$$\xi(\phi) = \left(\frac{\phi}{M_P} \right). \quad (39)$$

We assume simple power law models for the scalar field functions with proper normalization. These models are mostly used in the inflationary epoch where the “slow-roll” conditions are assumed to hold true. The “slow-roll” approximation neglects the most slowly changing terms in the equations of motion. However, during the late era, one can take fields that do not obey the slow-roll conditions. It is known that theories which involve Gauss–Bonnet terms coupled with an arbitrary scalar field produce gravitational waves which propagate with a velocity that deviates from the speed of light [89]. However, the recent GW170817 event has predicted that the primordial gravitational wave speed must be equal to the speed of light [99]. This leads to an incompatibility in the theoretical framework involving Gauss–Bonnet terms. If the theory considered is described by massless gravitons throughout the evolution of the universe, then this problem can be removed [89]. This implies that the scalar coupling function should satisfy the differential equation $\ddot{\xi} = H\dot{\xi}$. The Hubble parameter is obtained from the Friedmann equations which in turn connects the two scalar functions $V(\phi)$ and $\xi(\phi)$ in such a way that the differential equation is satisfied. In this paper we start from arbitrary forms of the scalar field coupling functions.

In the Einstein gravity $f(R) = R$ with GB terms, we do not have \dot{R} in the field equation, and the second derivative of the density parameter Ω_H is zero. However, the second derivative of the scalar field ϕ is proportional to Ω_H' as seen from the continuity equation. So, we need only one initial condition for Ω_H to solve the field equations (15) and (16). We assume that $\Omega_H|_{(z=0)} = \frac{\Lambda}{3m^2} \left(1 + \frac{1+z_f}{1000} \right)$ and the initial values for the scalar field are taken as $\phi|_{(z=0)} = 10^{-10} M_P =$

$\frac{d\phi}{dz}|_{(z=0)}$. The choice of the initial conditions are done in such a way so that they lead to a physically viable description of the present observed universe. We consider two types of interaction among the fluids where energy flows from the non-relativistic matter sector to the dark energy sector and vice versa, and summarize the results below.

Case-I: For $\eta > 0$ (i.e., $Q > 0$)

At first, we consider the case of energy transfer from the non-relativistic matter sector. The interaction coupling parameter η plays a crucial role in determining the stability of the model. For a suitable choice of the model parameters, the field equations are solved numerically and we have plotted the cosmological parameters in Fig. 1 for $\alpha = 0.9$ and $\eta = 0.0004$. From the figure, it is evident that the DE oscillations are absent in the case of $f(R) = R$ gravity, and as a consequence, all the cosmological parameters are oscillation free throughout the evolution of the universe. The scalar field in this case exhibits a monotonically decreasing nature and attains large negative values at the present epoch. The deceleration parameter shows a change in sign indicating a transition from a decelerating to an accelerating phase of expansion. The parameter Ω_H remains constant throughout. We note that the jerk and snap parameters approach their corresponding Λ CDM limits at $z \sim 0$ (Table 1).

In Table 1 we display the present day values of the cosmological parameters as obtained from the theoretical model and compare them with the PLANCK 2018 results [102]. We note that for the present model the cosmological parameters are close to their corresponding Λ CDM values at the present epoch. The DE variables i.e., the DE density parameter and the effective EoS parameter are plotted in Fig. 2. From the figure it is evident that Ω_{DE} increases as the universe enters the DE dominated phase. The effective EoS parameter in this case remains almost constant showing a slight deviation from the corresponding Λ CDM value. In the case of $R + GB$ gravity with scalar potential, we note that stable cosmological models are found for small values of the interaction parameter η . As η is increased, the snap parameter shows a discontinuity at certain redshifts making the model unstable. Further, decreasing α increases the allowed range of η values. So, the presence of the simple $f(R) = R$ gravity with a scalar potential leads to a universe DE oscillations. The universe in the modified gravity scenario with a scalar field resembles closely the Λ CDM model near $z = 0$. The DE EoS parameter indicates a phantom type DE dominated universe. This is different from the result obtained in Paul et al. [103].

Case-II: For $\eta < 0$ (i.e., $Q < 0$)

For $Q < 0$, i.e., the energy flow from the dark energy sector, one obtains similar behaviour as the previous case. For large negative values of η the jerk parameter however

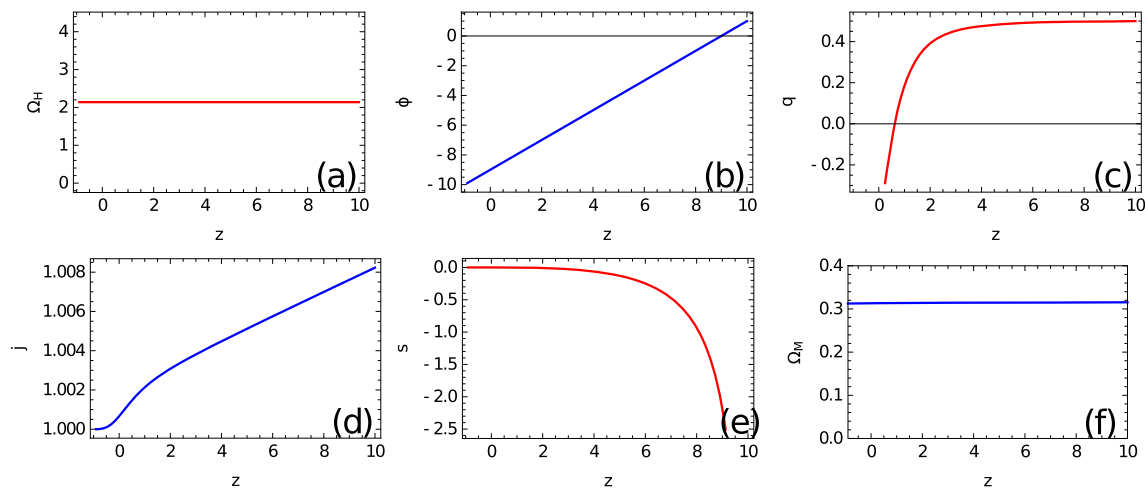


Fig. 1 Solutions for the statefinder parameter Ω_H and scalar field ϕ over reduced Planck mass with interaction considering $\alpha = 0.9$ and $\beta = 0.0004$ in presence of a scalar field $V(\phi)$. Cosmological parameters are also plotted as functions of redshift z

Table 1 Cosmological parameter values at the present epoch for $Q > 0$, with $\alpha = 0.9$ and $\eta = 0.0004$

Parameter	$R + V(\phi)$	ΛCDM
$q(z = 0)$	-0.521987	-0.535
$j(z = 0)$	1.00066	1
$s(z = 0)$	-0.0002167	0
$Om(z = 0)$	0.313387	0.3153 ± 0.07
$\Omega_{DE}(0)$	0.681461	0.6847 ± 0.0073
$w_{DE}^{eff}(0)$	-1.00036	-1.018 ± 0.031

Table 2 Cosmological parameter values at the present epoch for $Q > 0$, with different η and $\alpha = 0.9$

Parameter	$f(R)$ with $\eta = 0.006$	ΛCDM
$q(z = 0)$	-0.870821	-0.535
$j(z = 0)$	1.13689	1
$s(z = 0)$	-0.0332856	0
$Om(z = 0)$	0.322417	0.3153 ± 0.07
$\Omega_{DE}(0)$	0.916328	0.6847 ± 0.0073
$w_{DE}^{eff}(0)$	-1.00321	-1.018 ± 0.031
Parameter	$f(R)$ with $\eta = 0.06$	ΛCDM
$q(z = 0)$	-0.863784	-0.535
$j(z = 0)$	0.945195	1
$s(z = 0)$	0.013395	0
$Om(z = 0)$	0.340152	0.3153 ± 0.07
$\Omega_{DE}(0)$	0.916371	0.6847 ± 0.0073
$w_{DE}^{eff}(0)$	-1.05092	-1.018 ± 0.031

diverges near $z = 0$ thus making the model unstable. The DE oscillations are absent in this case too, and as a result, the statefinder parameters are also oscillation free. We plot the

results in Fig. 3. In this case, the DE stays in the quintessence region. We note that stable cosmological models can be constructed in this case when the DE interacts only with the non-relativistic matter sector which was not possible in case of a three fluid interaction scenario [103].

4.2 Model-II

For the second model, simple forms of the scalar field coupling function $\xi(\phi)$ and the potential $V(\phi)$ are considered. The primordial GW speed puts a strict constraint on the forms of these functions [89], and here we consider a finite GW speed and a free scalar field. Thus, in absence of the scalar potential ($V(\phi) = 0$) the GB coupling term is considered as:

$$\xi(\phi) = e^{\frac{\phi}{M_P}} \tag{40}$$

The $f(R)$ function is considered to be of the form:

$$f(R) = R + \left(\frac{R}{M}\right)^2 - \lambda \left(\frac{R}{3m_s^2}\right)^\delta \tag{41}$$

where, λ (dimensions of mass squared) and δ are constants. Here M is approximately equal to $M = 1.5 \times 10^{-5} \left(\frac{50}{N}\right) M_P$, with N being the number of e -foldings and the exponent δ is positive in the interval $0 < \delta < 1$.

This functional form of $f(R)$ is considered here as it can give a reasonable description of the inflationary epoch as well as the late time era [89, 103]. The model is also well known for producing dark energy oscillations in the high redshift regions. The R^2 term dominates the dynamical evolution in the early epoch, when R is large and controls the inflationary behaviour, whereas the R^δ term dominates during the present

Fig. 2 Variation of dark energy variables, the effective EoS parameter w_{DE}^{eff} (Right) and Density parameter Ω_{DE} (Left) with interaction considering $\alpha = 0.9$ and the $\beta = 0.0004$

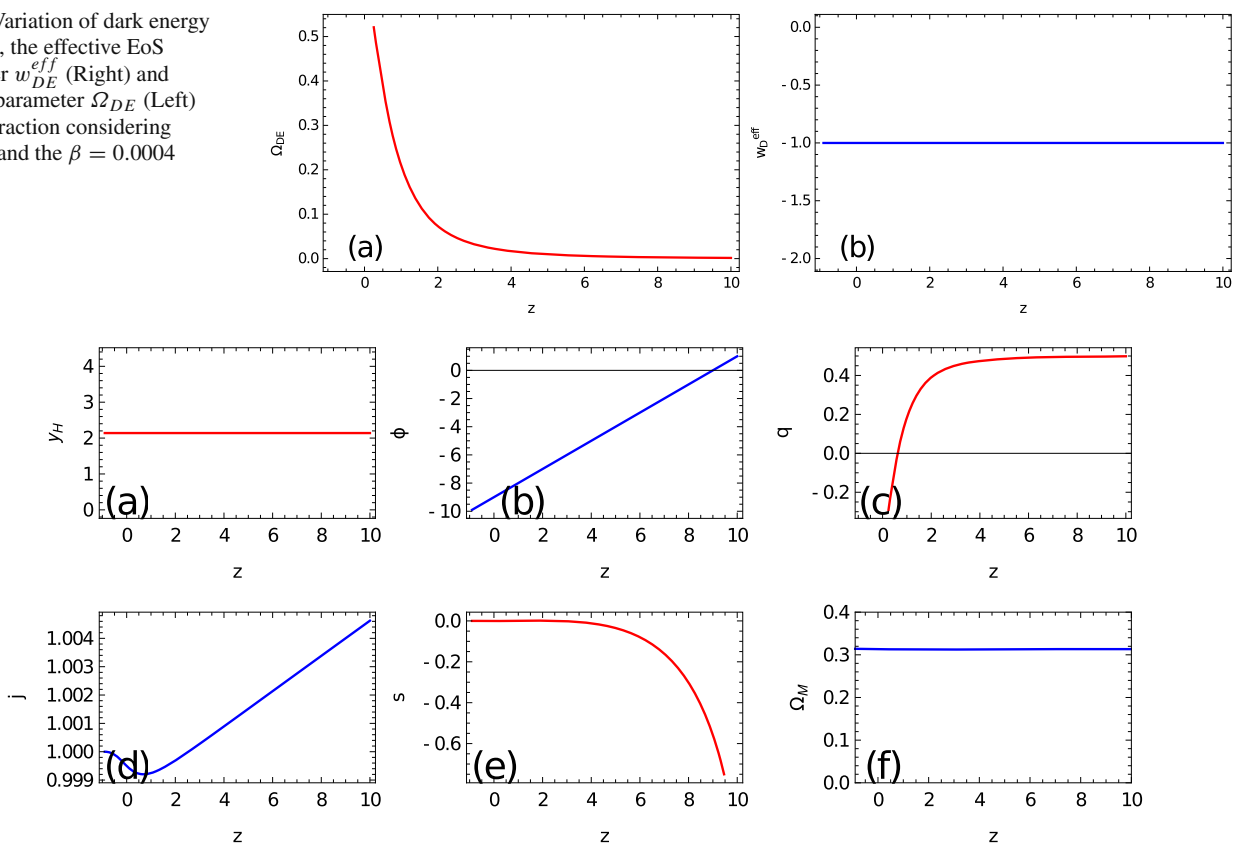


Fig. 3 Solutions for the statefinder parameter Ω_H and scalar field ϕ over reduced Planck mass with interaction considering $\alpha = 0.9$ and $\eta = -0.0006$ in presence of a scalar field $V(\phi)$. Cosmological parameters are also plotted as functions of redshift z

epoch with $R \rightarrow 0$ for $\delta < 1$. The presence of the scalar field further alters the dynamics of the evolving universe.

In the literature, cosmological models with this functional form of $f(R)$ have been studied earlier. The dynamics of evolution of the late universe is studied by Odintsov et al. in presence of string theory motivated axion like particles and in the presence of a scalar field coupled GB term [89, 92–94]. It is found that although Gauss–Bonnet terms alone can produce oscillation free dark energy era, in presence of $f(R)$ gravity one cannot avoid DE oscillations in the high redshift domain indicating that $f(R)$ gravity dominates over the GB term [104]. Motivated by this result, Paul et al. [103] studied the late-time evolution of the universe in the $f(R)$ gravity with GB terms, considering interacting three fluids model. In the model, the role of interaction that sets in among the fluid components are investigated. A linear interaction was considered and they found that even with interactions among the fluid components the DE oscillations still exist in the high redshift domain. They found that as the strength of the interaction is increased the DE oscillations smooths out but it leads to singularities in the statefinder parameters at some particular redshifts. Thus, singularity free stable cosmological models cannot be realized without DE oscillations for the specific $f(R)$ gravity under consideration [103].

In the present work, a scalar field is considered with a non-linear interaction between the cosmic fluid components to examine the role of interaction on the late-time evolutionary features of the universe. The role of such an exponential interaction between the dark sectors has been studied in the literature in a GR framework [83]. Different observational data have been used to constrain the strength of interaction and it is found that the model is in agreement with the observations for small values of the parameter η . At the background level, the cosmological model is found to resemble the Λ CDM model with a slight deviation under small perturbation when CMB temperature anisotropy is considered. We probe here the exponential interaction between the non-relativistic matter sector and the DE sector in a $f(R) + GB$ gravity framework to study late universe in the presence of interaction.

We consider a set of values of the model parameters $\lambda = 118.895 \times 10^{-67} \text{ eV}^2$, $\delta = 10^{-2}$ and $N = 60$ e-folding which lead to a physically consistent cosmology. The current value of the Hubble parameter is taken from the Planck data which is, $H_0 = 67.4 \text{ km/s/Mpc}$ [102], which when converted in the unit of eV becomes $H_0 = 1.37187 \times 10^{-33} \text{ eV}$. Equations (15) and (16) are analyzed numerically considering suitable initial conditions for a range of redshifts that

describe the last stages of the matter domination epoch up to the present time, i.e., $[z_i, z_f] = [0, 10]$. The initial conditions are considered to be [89],

$$\begin{aligned}\Omega_H \Big|_{(z=10)} &= \frac{\lambda}{33m_s^2} \left(1 + \tilde{\gamma}(1 + z_f) \right), \\ \frac{d\Omega_H}{dz} \Big|_{(z=10)} &= \tilde{\gamma} \left(\frac{\lambda}{33m_s^2} \right), \\ \phi \Big|_{(z=10)} &= 10^{-16} M_P, \quad \frac{d\phi}{dz} \Big|_{(z=10)} = -10^{-17} M_P, \quad (42)\end{aligned}$$

which gives a viable description of the present observed universe. The parameter $\tilde{\gamma}$ is a dimensionless entity that acts as a free parameter. The initial conditions assumed here, play an important role in the dynamical evolution of the universe. The nature of the evolution of the cosmological parameters depend on the initial conditions through $\tilde{\gamma}$ which will be discussed in the following. We consider $\tilde{\gamma} = 10^{-3}$ for the rest of the manuscript as it yields a reasonable phenomenological behaviour of the cosmological parameters, however, it can assume higher values also in principle. The accurate forms for the initial conditions may however be obtained considering some cosmographic approach which is beyond the scope of the present paper and will be tackled elsewhere. We consider two different scenarios where the energy flows from the non-relativistic matter sector to the dark energy sector and vice versa.

Case-I: For $\eta > 0$ (i.e., $Q > 0$)

For the first case, we consider $\eta > 0$ ($Q > 0$) i.e. the energy flow from the non-relativistic matter sector to the other two fluids. The system of Eqs. (15), (16) and (37) are analyzed numerically considering suitable values of the model parameters. We plot the variation of different cosmological parameters with the redshift z in Fig. 4 for a specific choice of α and η . From Fig. 4a it is evident that for the chosen values of the model parameters one cannot nullify the DE oscillations for $z \geq 3$ in the interacting $f(R) + f(\mathcal{G})$ gravity. The scalar field is found to be free from oscillations and increases as the universe enters the DE dominated epoch as shown in Fig. 4b. The variation of the deceleration parameter (q), jerk parameter (j), snap parameter (s) and $Om(z)$ parameter with the redshift z are shown in Fig. 4c–f. For $\eta = 0.006$ and $\alpha = 0.9$, the oscillating nature prevails at higher redshifts. However, the oscillations smooths out considerably near the present epoch ($z = 0$). The deceleration parameter shows a flip in sign indicating a transition from a decelerated phase of expansion to an accelerated phase of expansion of the present universe. The transition redshift (redshift at which the universe enters the accelerated phase of expansion) depends on the type of interaction and the initial conditions which will be discussed in the following. The statefinder pair j and s approach their corresponding Λ CDM values ($j = 1, s = 0$) at the present epoch. The $Om(z)$ parameter shows a clear

distinction between the present model (blue, solid) and the Λ CDM (black, dot dashed) [102]. Even at very low redshifts this distinction is pretty evident as seen from Fig. 4f. We have compared the present values of different cosmological parameters obtained from our model with the observed results in Table 2.

In Fig. 5 we plot the evolution of the effective DE EoS parameter (w_{DE}^{eff}) and the DE density parameter (Ω_{DE}). Both of these parameters exhibit oscillating nature at high redshifts. We note from Fig. 5 that for high redshifts ($z \sim 10$), the effective DE EoS parameter shows oscillations which is an indication of the transfer of energy from one sector of matter to the others. At the present epoch, the oscillations die out reaching a stable configuration with a negative EoS parameter indicating the existence of exotic matter obtained from the transformation mechanism in a modified gravity scenario with interacting fluids.

The oscillating behaviour of the cosmological parameters is a direct consequence of the dominance of the $f(R)$ gravity part over the Gauss–Bonnet terms. However, the interaction between the fluids plays a crucial role in this case. We note that as the interaction strength is increased beyond a certain point the DE oscillations cease to exist. For $\alpha = 0.9$, oscillations vanish around $\eta = 0.38$. However, in this case, the statefinder parameter s shows a discontinuous behaviour at a certain redshift which is not desirable for a stable cosmological model. This behaviour is shown in Fig. 6. Thus one can estimate the range of the strength of interaction leading to a stable cosmological model. In this work, we consider three different α values and determined the range of η numerically for a stable cosmological model.

In Fig. 7 we consider two different $\tilde{\gamma}$ values namely, $\tilde{\gamma} = 10^{-3}$ and $\tilde{\gamma} = 0.5$ to study the dependence of initial conditions on the DE oscillations. We plot the density parameter Ω_H and the deceleration parameter q for the $\tilde{\gamma}$ values considered. We note that the DE oscillations are more pronounced for $\tilde{\gamma} = 10^{-3}$. However, the present behavior of these parameters become independent of the initial conditions. The transition redshift also changes with the choice of $\tilde{\gamma}$.

Case-II: For $\eta < 0$ (i.e., $Q < 0$)

For $Q < 0$, the energy flows from the DE sector. In a similar way to the earlier case, we analyze the system of equations numerically. The results are shown in Fig. 8. The parameter Ω_H is again found to be oscillating in the past, and thereafter at the present epoch, the oscillations die out attaining a constant value. The behaviour of the scalar field is similar to the previous case where it gradually increases attaining a maximum at the present epoch. Thus we conclude that the behaviour of the scalar field is independent of the direction of energy flow. The evolution of the cosmological parameters are shown in Fig. 8c–f. The statefinder parameters in this case exhibit oscillations for higher redshifts ($z \sim 3$) similar

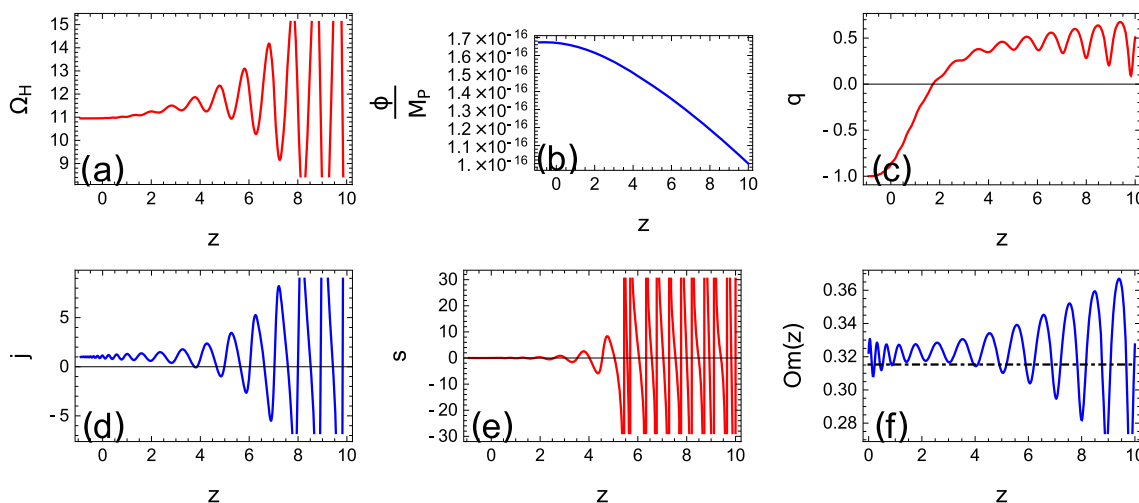
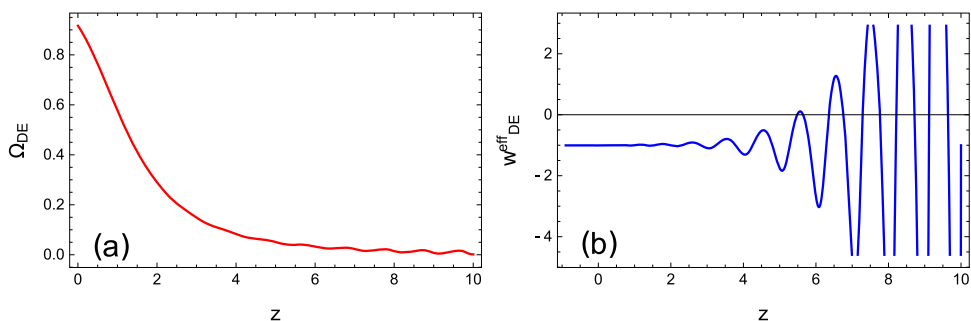


Fig. 4 The density parameter Ω_H and scalar field ϕ over reduced Planck mass for the $f(R)$ gravity with interaction considering $\eta = 0.006$ and $\alpha = 0.9$. Other cosmological parameters are also plotted as functions of redshift parameter z

Fig. 5 Variation of dark energy variables, the effective EoS parameter w_{DE}^{eff} (right) and Density parameter Ω_{DE} (left) with interaction considering $\eta = 0.006$ and $\alpha = 0.9$



to the previous case. We plot the figures for $\alpha = 0.9$ and $\eta = -0.006$. We note that for large negative values of the interaction strength η the DE oscillations vanish. However, as before, the cosmological parameters exhibit singularity at a certain redshift, thus making the model unstable.

The dark energy density parameter and the effective EoS parameter are plotted in Fig. 9. The effective EoS parameter is oscillating at high redshifts, but the oscillations damp down and the EoS parameter approaches the quintessence value. The difference between these two cases is that in the previous case the DE turns out to be in the phantom region at the present epoch, whereas for $Q < 0$ it stays in the quintessence region. For smaller η values the difference between the present day values of w_{DE}^{eff} for $Q > 0$ and $Q < 0$ is negligible, however, as η is increased within the permissible range, the difference becomes significant. We have estimated the present day values of the cosmological parameters for $\eta = \pm 0.006$ and $\eta = \pm 0.06$ in Tables 2 and 3. It is evident from these two tables that for larger η values one can distinguish between the two cases $Q > 0$ and $Q < 0$ by determining the type of DE present in the universe. We note that for higher redshifts there was a transformation between the phantom and quintessence type of DE in both cases. As the universe approached the present epoch ($z \sim 0$), the oscil-

lation gets damped significantly and a stable configuration is reached. For $Q > 0$, the nature of DE remains in the phantom domain whereas for $Q < 0$ it stays in the quintessence region.

Next, we study the effect of linear and exponential interaction on the dynamics of the evolution of the universe. For $\alpha = 1$, the interaction reduces to a linear form. We compare the new density parameter Ω_H , the deceleration parameter q , and the effective EoS parameter w_{DE}^{eff} in both cases, and the results are plotted in Fig. 10. From the figure, we note that for the exponential interaction with higher order terms, the DE oscillations are less prominent, however, in both the interaction types Ω_H behave similarly in the present epoch. The universe transits into an accelerating phase faster when exponential interaction is taken up. Both the interactions indicate the presence of phantom type DE at the present universe with $Q > 0$ whereas they stay in the quintessence region for $Q < 0$. Thus one can conclude that the direction of energy flow determines the type of DE in the present universe rather than the type of interaction.

We further perform a comparison of the scenarios with and without interactions between the cosmic fluid components. In Fig. 11, the parameters Ω_H , q and w_{DE}^{eff} are plotted with redshift z in the presence and absence of interactions among the

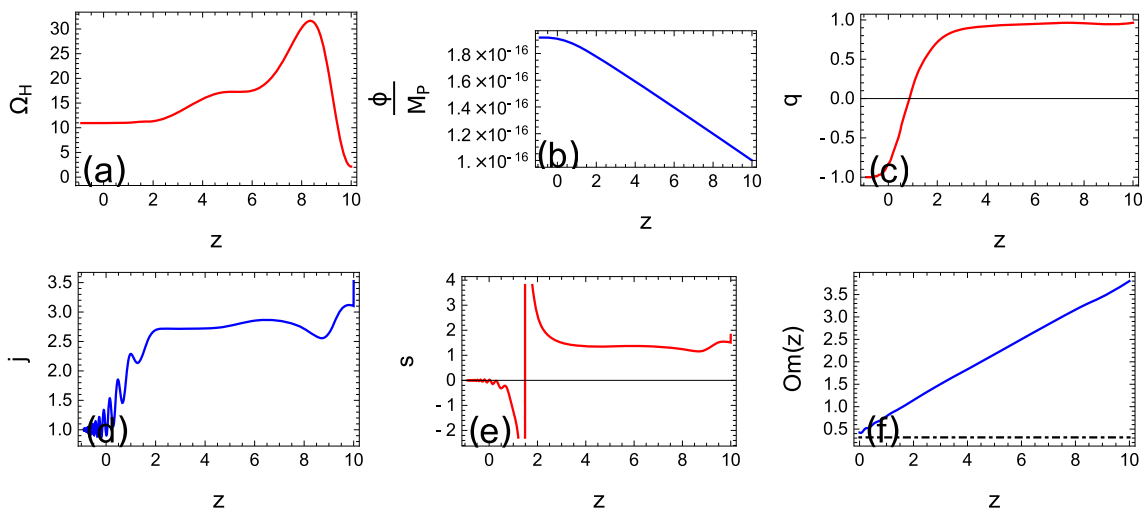


Fig. 6 Solutions for the density parameter Ω_H and scalar field ϕ over reduced Planck mass for the $f(R)$ gravity with interaction considering $\alpha = 0.9$ and $\eta = 0.38$. Cosmological parameters are also plotted as functions of redshift parameter z

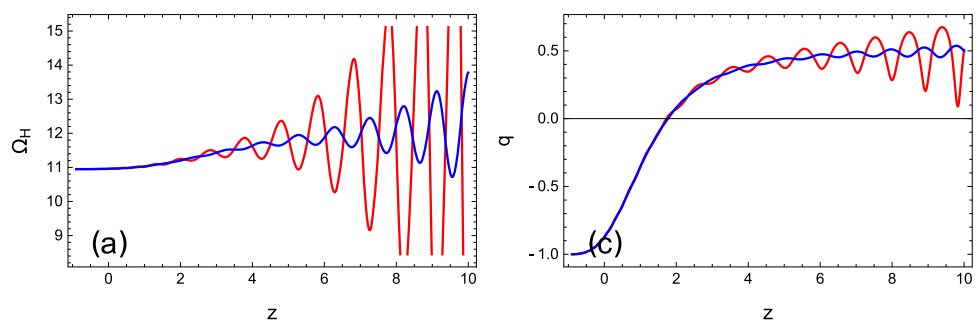
cosmic fluid components. From the figure, we note that the oscillating nature of the DE variables persists even without interaction, and for $\eta > 0$, the amplitude of DE oscillations is greater than the non-interacting scenario which lies between the $\eta > 0$ and $\eta < 0$ case. The transition redshift also shows a similar behaviour where the universe transits from a decelerating phase to an accelerating phase earlier in the case of $\eta < 0$. The transition for the non-interacting case is slower compared to the $\eta < 0$ case but faster than the $\eta > 0$ scenario. The plot of the effective DE EoS parameter clearly indicates that for the non-interacting scenario the effective EoS parameter stays close to -1 resembling the Λ CDM model. Thus the coupled fluid model alters the dynamics of evolution of the universe but, it cannot change the nature of evolution of the DE variables which continue to oscillate even in presence of interaction. This in turn indicates that the phenomenology of the late universe is mostly governed by the $f(R)$ gravity.

We have compared the present day values of the cosmological parameters for both the interaction types and the values are tabulated in Table 4. We note that the difference between these values are much less compared to the Λ CDM model or a cosmological model without interacting fluids. Thus $f(R)$ modified gravity dominates over the Gauss–Bonnet terms as

we observe oscillation of dark energy in the late time universe in the presence of interaction between the fluids. The interacting cosmic fluids play an important role in determining the evolutionary pattern of the universe. The existence of oscillation in the density parameter Ω_H for $z \geq 4$ imposes an upper bound on the strength of interaction η for a given α . Beyond this bound, discontinuities can appear in the cosmological parameters at a given redshift in the late time universe. Paul et al. recently studied the effect of linear interaction in a modified $f(R)$ gravity framework with GB terms and they observed that for a stable cosmological model, DE oscillations cannot be suppressed even with interacting fluids [103]. From the above analysis, it is evident that even with an exponential type of interaction between the cosmic fluid components, one cannot nullify the DE oscillations in the late universe. The allowed range of η for different α values are displayed in Table 5.

In Fig. 12a, b, the evolutions of different cosmological parameters are shown as well as their mutual dependences. The parametric representation of $Om(z)$ and $j(z)$ is plotted in Fig. 12a for different sets of model parameter η and α . From this figure it can be seen that for each chosen sets of model parameters, the plot exhibits an attractor like nature

Fig. 7 Solutions for the density parameter Ω_H and the deceleration parameter q for the $f(R)$ gravity with interaction considering $\eta = 0.006$ and $\alpha = 0.9$. The red curves correspond to $\tilde{\gamma} = 10^{-3}$ and the blue curves correspond to $\tilde{\gamma} = 0.5$



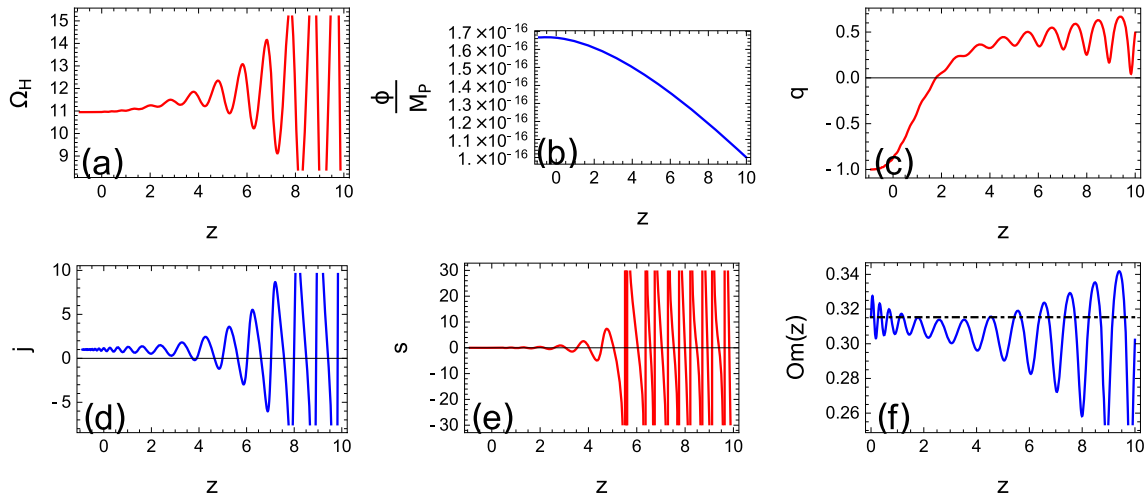


Fig. 8 Evolution of the density parameter Ω_H and scalar field ϕ for the $f(R)$ gravity with GB terms and interacting fluids taking $\alpha = 0.9$ and $\eta = -0.006$. Cosmological parameters are also plotted as functions of redshift z

Fig. 9 Variation of dark energy variables, the effective EoS parameter w_{DE}^{eff} (right) and Density parameter Ω_{DE} (left) with interaction considering $\alpha = 0.9$ and $\eta = -0.006$

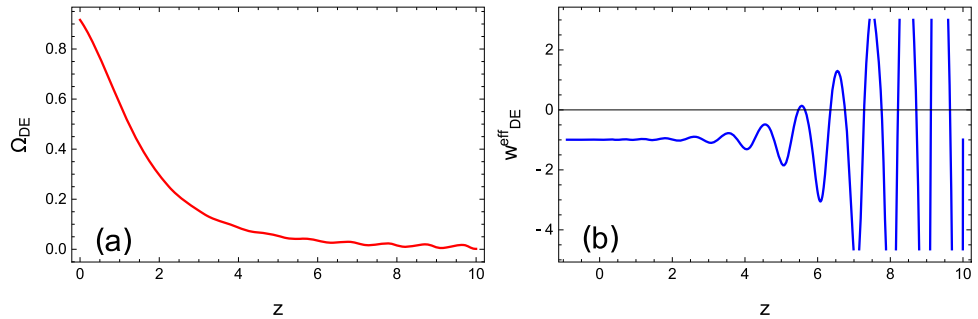


Table 3 Cosmological parameter values at the present epoch for $Q < 0$, with different η and $\alpha = 0.9$

Parameter	$f(R)$ with $\eta = -0.006$	ΛCDM
$q(z = 0)$	-0.873596	-0.535
$j(z = 0)$	1.15176	1
$s(z = 0)$	-0.036827	0
$Om(z = 0)$	0.315478	0.3153 ± 0.07
$\Omega_{DE}(0)$	0.916325	0.6847 ± 0.0073
$w_{DE}^{eff}(0)$	-0.993486	-1.018 ± 0.031
Parameter	$f(R)$ with $\eta = -0.06$	ΛCDM
$q(z = 0)$	-0.884884	-0.535
$j(z = 0)$	1.11436	1
$s(z = 0)$	-0.027525	0
$Om(z = 0)$	0.287331	0.3153 ± 0.07
$\Omega_{DE}(0)$	0.916333	0.6847 ± 0.0073
$w_{DE}^{eff}(0)$	-0.948815	-1.018 ± 0.031

and evolves toward a stable point near $j(z) \approx 0$ (but different values of $Om(z)$). The corresponding nature of the deceleration parameter $q(z)$ can be observed in Fig. 12b, where the evolutions of $q(z)$, $j(z)$ and $Om(z)$ are simultaneously plot-

ted in 3d parametric space. From Fig. 12b it can be observed that $q(z)$ oscillates with z at higher redshifted era. However as two other parameters $j(z)$ and $Om(z)$ move toward stable points, the oscillating nature of $q(z)$ diminishes and the value of $q(z)$ start decreasing rapidly.

Finally, the velocity of the primordial gravitational waves can be calculated for both the model, which is given by [105–107]:

$$c_T^2 = 1 - \frac{Q_f}{2Q_t} \tag{43}$$

where, $Q_f = 16(\ddot{\xi} - H\dot{\xi})$ and $Q_t = M_p^2 - 8\dot{\xi}H$. The gravitational wave speed can assume arbitrary values depending on the scalar field coupling function $\xi(\phi)$. However, despite being arbitrary, its value is close to unity as $Q_f \ll Q_t$. The variation of the GW speed with the redshift parameter is plotted in Fig. 13 for a given interaction strength considering both models. It is evident from the figure that in both cases the GW wave speed is close to unity. For the second model we consider $\alpha = 0.9$ and $\eta = 0.006$, the value of Q_f is of the order $Q_f \sim 10^{-82}$ whereas $Q_t \sim 10^{-29}$ and hence, the ratio is very close to zero. This leads to a GW speed close to unity which is consistent with the GW170817 event. From the expression of Q_f , one can see that as $Q_f \rightarrow 0$,

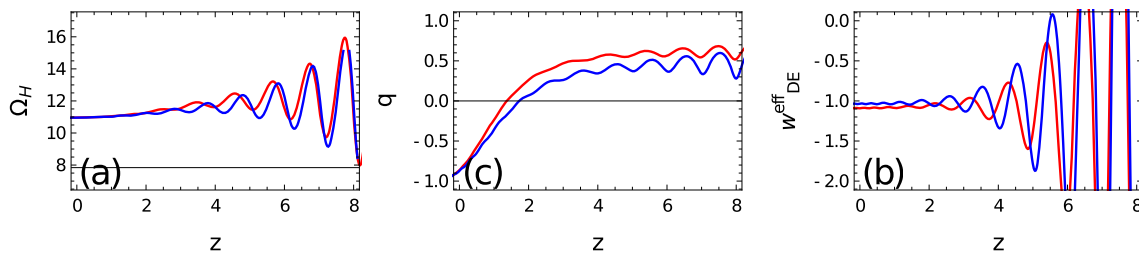


Fig. 10 Variation of dark energy variables, Ω_H (left), deceleration parameter q (middle) and the effective EoS parameter w_{DE}^{eff} (right) with exponential interaction (blue) and with linear interaction (red) considering $\eta = 0.09$ and $\alpha = 0.1$

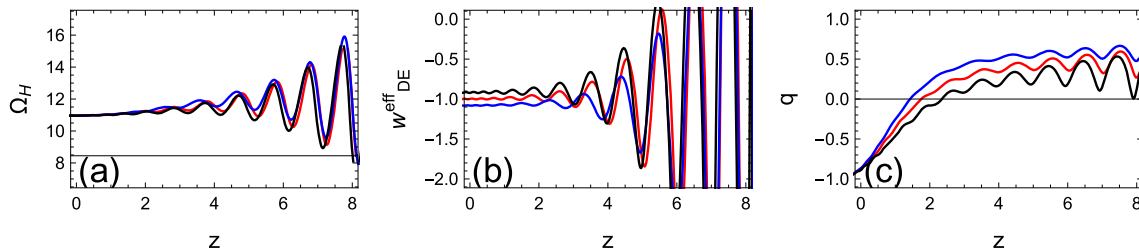


Fig. 11 Variation of dark energy variables, Ω_H (left), deceleration parameter q (right) and the effective EoS parameter w_{DE}^{eff} (middle) with and without interaction. The red curve corresponds to the non-interacting scenario and the blue and black curves correspond to $\eta = \pm 0.09$ and $\alpha = 0.9$ respectively

Table 4 Cosmological parameter values at the present epoch for $Q < 0$, with exponential and linear interaction

Parameter	Exponential interaction	Linear interaction
$q(z = 0)$	-0.872836	-0.887245
$j(z = 0)$	1.14922	1.0965
$s(z = 0)$	-0.036229	-0.023188
$Om(z = 0)$	0.317226	0.281453
$\Omega_{DE}(0)$	0.916325	0.916337
$w_{DE}^{eff}(0)$	-0.974235	-0.943802

Table 5 Constraints on the interaction parameter η for different fluid interactions

Types of Interaction	α	η
$Q > 0$	$\alpha = 0.9$	$0 \leq \eta \leq 0.38$
	$\alpha = 0.7$	$0 \leq \eta \leq 0.59$
	$\alpha = 0.5$	$0 \leq \eta \leq 0.97$
$Q' < 0$	$\alpha = 0.9$	$-1.2 \leq \eta \leq 0$
	$\alpha = 0.7$	$-1.91 \leq \eta \leq 0$
	$\alpha = 0.5$	$-3.11 \leq \eta \leq 0$

5 Observational viability

We compare our model with UNION 2.1 data [108]. The UNION 2.1 data contains the information of 580 type Ia (SnIa) Supernovae, in the form of distance modulus μ_{obs} of individual supernova along with their error bounds σ_μ and the redshift z . The distance modulus μ is related to the luminosity distance as,

$$\mu = m - M = 5 \log D_L + \mu_0, \tag{44}$$

where m, M are the apparent and absolute magnitudes of the Supernovae respectively, and $\mu_0 = 5 \log \left(\frac{H_0^{-1}}{M_{pc}} \right) + 25$ is a nuisance parameter which is marginalized. Distance modulus D_L for an object placed at redshift z is given by,

$$D_L(z) = (1 + z) \int_0^z \frac{H_0 dz'}{H(z')}. \tag{45}$$

Now, in order to compare our calculated distance modulus μ_{th} with the observed distance modulus μ_{obs} , another parameter χ_{SN}^2 is introduced, which represents the mean square deviation from the observed data. The parameter χ_{SN}^2 can be defined as,

$$\chi_{SN}^2(\eta, \alpha) = \sum_{i=1}^{580} \frac{(\mu_{th}(z_i, \mu_0, \eta, \alpha) - \mu_{obs}(z_i))^2}{\sigma_\mu(z_i)^2}. \tag{46}$$

$\ddot{\xi} = H\dot{\xi}$. Thus, the GB coupling parameter is important and the choice of the scalar coupling function to the GB terms is not arbitrary.

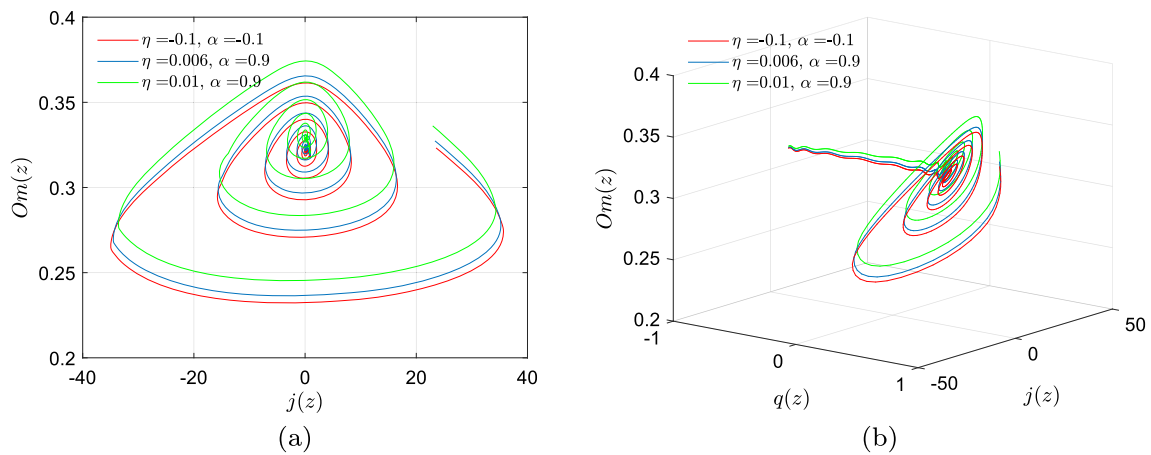


Fig. 12 **a** Evolution of $q(z)$ and $j(z)$ for different values of η and α in the case of model I. **b** Parametric representation of $q(z)$, $j(z)$ and $Om(z)$ for different chosen sets of model parameters η and α in the case of model I

Fig. 13 Variation of the gravitational wave speed with redshift parameter z for model I with $\alpha = 0.9$ and $\eta = 0.0006$ and model II with $\alpha = 0.9$ and $\eta = 0.006$

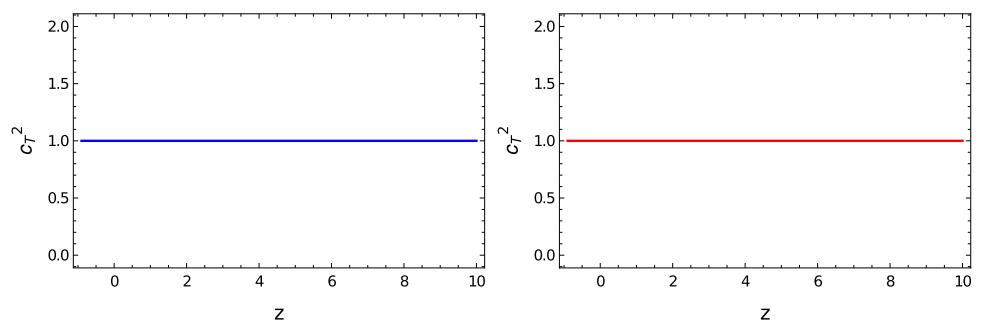
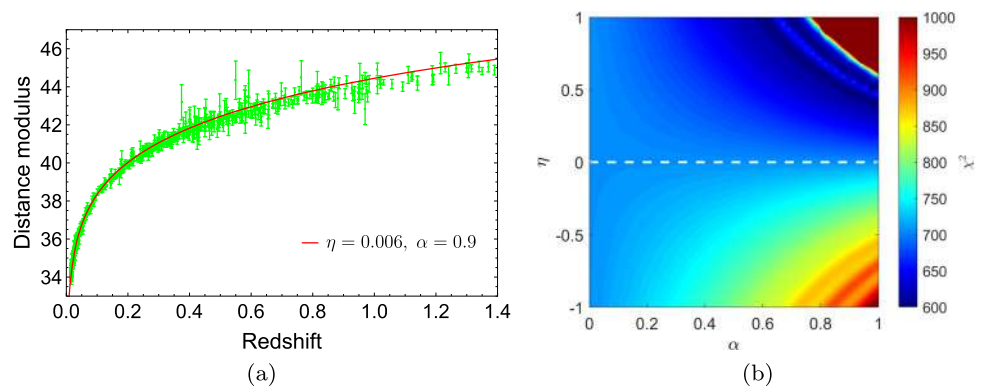


Fig. 14 **a** Comparison of model I with Union 2.1 supernova data while the model parameters chosen at $\eta = 0.006$, $\alpha = 0.9$. **b** χ^2 representation of model I in $\eta - \alpha$ parameter plane using Union 2.1 supernova data. In this plot the while dashed line corresponds to the case of $\eta = 0$



However, to get rid of μ_0 , one can redefine χ_{SN}^2 as [109,110],

$$\chi_C^2(\eta, \alpha) = \sum_{i=1}^{580} \frac{1}{\sigma_{\mu}(z_i)^2}. \tag{50}$$

$$\chi_{SN}^2(\theta) = \chi_A^2 - \frac{\chi_B^2}{\chi_C^2}. \tag{47}$$

where $\chi_A^2(\eta, \alpha)$, $\chi_B^2(\eta, \alpha)$ and $\chi_C^2(\eta, \alpha)$ are given by

$$\chi_A^2(\eta, \alpha) = \sum_{i=1}^{580} \frac{(\mu_{th}(z_i, \mu_0, \eta, \alpha) - \mu_{obs}(z_i))^2}{\sigma_{\mu}(z_i)^2}, \tag{48}$$

$$\chi_B^2(\eta, \alpha) = \sum_{i=1}^{580} \frac{\mu_{th}(z_i, \mu_0, \eta, \alpha) - \mu_{obs}(z_i)}{\sigma_{\mu}(z_i)^2}, \tag{49}$$

From Fig. 14a, it can be seen that the model fits well with the Union 2.1 supernova data, where the model parameters are chosen at $\eta = 0.006, \alpha = 0.9$. The variation of χ_{SN}^2 for different model parameter η and α are graphically represented in Fig. 14b. In this figure (Fig. 14b) it is observed that, the parameters values near the dark blue region at higher α and η fit the best with observational data. From this plot one can conclude that the model is not observationally viable in the region $[\alpha \approx 1, |\eta| \geq 0.5]$. In Fig. 14b, the white dashed line represents the case of $\eta = 0$. It can be seen that, at $\eta = 0$,

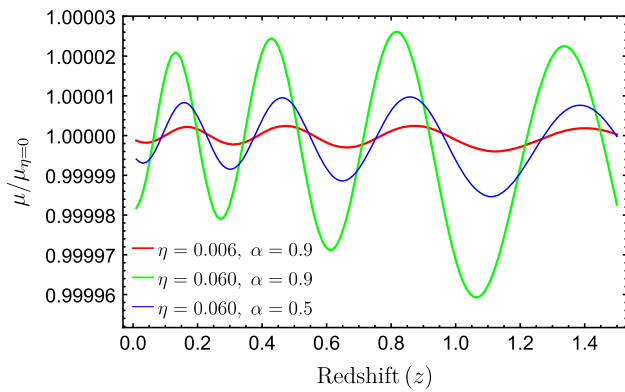


Fig. 15 Variation of distance modulus with redshift z for different chosen values of η and α . In this figure, the distance modulus (μ) is parametrized as $\mu/\mu_{\eta=0}$, where $\mu_{\eta=0}$ is distance modulus where the effect of fluid interaction is not considered

the variation of χ^2 value and hence the same distance modulus with α vanishes. This particular case ($\eta = 0$) denotes the condition, where the effect of fluid interaction is absent (Fig. 15).

6 Summary and conclusions

In this paper, we present late time cosmological models in $f(R)$ modified gravity with coupled Gauss–Bonnet terms. The background cosmic fluid is assumed to be composed of three different components, namely, the non-relativistic matter section which includes CDM also, relativistic matter components as well as dark energy. We consider an interacting two fluid scenario, where the non-relativistic matter section interacts with the dark energy. The relativistic particles do not take part in the interaction [89]. The strength of interaction between the cosmic fluid components plays an important role in determining the late time evolutionary dynamics of the universe. In this work we have considered an exponential form of interaction as it is the simplest generalization of the linear form, to study the effect of higher order terms on the background dynamics of the universe. For a specific choice of model parameters, the interaction effectively reduces to a linear form and thus, the effect of these two interactions on the cosmological parameters can be compared.

We have considered two different forms of the gravitational action as: (I) the Einstein–Hilbert form of action $f(R) = R$ with GB terms coupled with a scalar field in a self interacting potential, and (II) $f(R) = R + \left(\frac{R}{M}\right)^2 - \lambda\left(\frac{R}{3m_s^2}\right)^\delta$ with GB terms coupled in the presence of a dilaton field. The numerical analysis of our models indicates that for a suitable choice of model parameters, the accelerating universe is accommodated naturally. Different functional forms of inter-

actions are considered to study the role of interactions on the late time phenomenology.

For the Einstein gravity ($f(R) = R$) with GB terms coupled to a scalar field in a potential $V(\phi)$ we have obtained cosmological evolution in presence of interaction Q . The scalar field coupling function $\xi(\phi)$ and the potential $V(\phi)$ are chosen keeping in mind the GW speed constraint condition [89]. We consider two different interacting scenarios ($\eta > 0$ and $\eta < 0$) and study the dynamics of evolution of the late universe. We note that in both cases the DE oscillations are absent. For small values of the interaction parameter η , and $\eta > 0$, stable cosmological models can be obtained in this case. The EoS parameter remains constant throughout, deviating only slightly from the corresponding Λ CDM value. A similar behaviour can be observed for $\eta < 0$ when energy flows from the dark energy sector to the non-relativistic matter sector. We can thus conclude that for the Einstein gravity DE oscillations smooth out and the model closely corresponds to the standard model near $z \sim 0$.

For the second model we consider the $f(R)$ modified gravity with additional R^2 and R^δ terms where $\delta < 1$, is a small perturbative term. Such a functional form can accommodate the early inflation as well as the late time acceleration [108]. In the present work we consider a free scalar field ($V(\phi) = 0$) and study the evolution of the universe for two different interaction scenarios. The form of the GB coupling function is chosen in such a way as to satisfy the constraint on the GW speed [99]. Two different cases have been considered, as before, depending on the sign of the interaction coupling parameter η . For $\eta > 0$, we find that for high redshifts, the parameter Ω_H oscillates rapidly, though the oscillation gradually subsides as the universe enters the present epoch. Similar behaviour is observed for the other cosmological parameters, as well. The universe enters the accelerated phase of expansion near $z \sim 2$. The model approaches the Λ CDM limit near $z \sim 0$. The presence of the exponential interaction makes the DE oscillations more prominent in this case. One interesting thing to note here is that the model is permitted for small values of η ($\eta \sim 0$) which was also obtained for a GR background using MCMC simulations [83]. For the specific $f(R)$ model under consideration, one cannot get rid of DE oscillations for high redshifts even with exponential interaction between non-relativistic matter and dark energy.

The role of the parameter η is significant since the interaction strength cannot be increased indefinitely. There exists an upper limit of η beyond which stable cosmological models cannot be constructed. The evolutionary behaviour of the cosmological parameters is affected by the choice of initial conditions. The initial conditions can be chosen in such a way that the model becomes consistent with the PLANCK 2018 results [102]. The initial conditions also play a crucial role in determining the transition redshift. For $\eta < 0$, simi-

lar behaviour is observed regarding the cosmological parameters. One major difference between these two interaction scenarios is evident through the present day values of the effective DE EoS parameter. For $\eta > 0$ the EoS parameter indicates the presence of phantom DE, whereas for $\eta < 0$ the DE is of quintessence type at the present epoch. The difference is evident for large values of η within the permissible range. The model corresponds to the standard Λ CDM model at the present epoch up to a certain limit, however the difference between these two scenarios is evident from the plots of the $Om(z)$ parameter. The range of allowed interaction strength η has been estimated. For a specific α , stable singularity free cosmological models cannot be constructed beyond these specific η values.

Finally, we have compared our theoretical model with the observed data of type Ia supernovae (UNION 2.1 data). For the $f(R) = R + \left(\frac{R}{M}\right)^2 - \lambda\left(\frac{R}{3m_s^2}\right)^\delta$ gravity with scalar field coupled GB terms, the model fits well with the Union 2.1 supernova data for $\eta = 0.006$ and $\alpha = 0.9$ validating the choice of interaction parameters. For a general choice of the parameters η and α , we find that the model is not observationally viable in the region [$\alpha \approx 1$, $|\eta| \geq 0.5$].

To conclude, in the $f(R) = R + \left(\frac{R}{M}\right)^2 - \lambda\left(\frac{R}{3m_s^2}\right)^\delta$ gravity with GB term coupled with a free scalar field, cosmological models are permitted with oscillating statefinder parameters in the late time universe. The oscillations however smooth out considerably as the universe enters the present accelerating phase. The modified form of $f(R)$ has been studied with and without interactions among the cosmic fluid components in the literature, and DE oscillations exist for high redshifts even with GB terms and interacting fluid scenario [103]. In the present work, we have studied the late time phenomenology of the universe considering a two fluid interacting scenario with an exponential interaction form. We have shown that the oscillating nature of DE persists even with exponential interaction. The oscillations however disappear if one increases the strength of interaction η up to a certain point for a fixed α . From our analysis it is further evident that the Gauss–Bonnet term plays a somewhat sub-dominant role in the late time era as compared to the $f(R)$ gravity. Moreover, the constrained nature of the scalar field coupling functions ensures that the GW wave speed calculated from the model agrees with the observations [99, 103].

Acknowledgements AC would like to thank the University of North Bengal for awarding Senior Research Fellowship. BCP would like to thank SERB-DST for awarding a project (Project no. CRG/2021/000183). AC and BCP would like to thank IUCAA Centre for Astronomy Research and Development (ICARD), NBU for extending research facilities. We are thankful to the anonymous referee for suggestions to present the paper in its current form.

Data Availability Statement This manuscript has associated data in a data repository. [Authors' comment: The data associated with the

manuscript is publicly available. There is no DATA generated which is to be deposited.]

Open Access This article is licensed under a Creative Commons Attribution 4.0 International License, which permits use, sharing, adaptation, distribution and reproduction in any medium or format, as long as you give appropriate credit to the original author(s) and the source, provide a link to the Creative Commons licence, and indicate if changes were made. The images or other third party material in this article are included in the article's Creative Commons licence, unless indicated otherwise in a credit line to the material. If material is not included in the article's Creative Commons licence and your intended use is not permitted by statutory regulation or exceeds the permitted use, you will need to obtain permission directly from the copyright holder. To view a copy of this licence, visit <http://creativecommons.org/licenses/by/4.0/>.

Funded by SCOAP³. SCOAP³ supports the goals of the International Year of Basic Sciences for Sustainable Development.

References

1. A.G. Riess et al., *Astron. J.* **116**, 1009 (1998)
2. S. Perlmutter et al., *Astrophys. J.* **517**, 565 (1999)
3. Eisenstein et al., *Astrophys. J.* **633**, 560 (2005)
4. C.L. Bennett et al., *Astrophys. J.* **483**, 565 (1997)
5. D.N. Spergel et al., *Astrophys. J. Suppl.* **148**, 175 (2003)
6. D.N. Spergel et al., *Astrophys. J. Suppl.* **170**, 377 (2007)
7. V. Sahni, A.A. Starobinsky, *Int. J. Mod. Phys. D* **9**, 4 (2000)
8. P. Padmanabhan, *Phys. Rep.* **380**, 5–6 (2003)
9. P.J.E. Peebles, B. Ratra, *Rev. Mod. Phys.* **75**, 559 (2003)
10. E. Komatsu et al., *Astrophys. J. Suppl.* **180**, 330–376 (2009)
11. A.G. Riess et al., *Astrophys. J. Lett.* **908**(1), L6 (2021)
12. W.L. Freedman et al., *Astrophys. J.* **882**, 34 (2019)
13. W.L. Freedman et al., *Astrophys. J. Suppl.* **919**(1), 16 (2021)
14. W. Yuan et al., *Astrophys. J.* **886**, 61 (2019)
15. J. Soltis, S. Casertano, A.G. Riess, *Astrophys. J. Lett.* **908**(1), L5 (2021)
16. S.M. Carroll, *Living Rev. Relativ.* **4**, 1 (2001)
17. S. Nojiri, S.D. Odintsov, V.K. Oikonomou, *Phys. Rep.* **692**, 1 (2017)
18. S. Capozziello, M. De Laurentis, *Phys. Rep.* **509**, 167 (2011)
19. V. Faraoni, S. Capozziello, *Beyond Einstein Gravity: A Survey of Gravitational Theories for Cosmology and Astrophysics*, *Fundam. Theor. Phys.*, 170 (2010), (Springer, Dordrecht, 2011)
20. S. Nojiri, S.D. Odintsov, *Phys. Rep.* **505**, 59 (2011)
21. G.J. Olmo, *Int. J. Mod. Phys. D* **20**, 413 (2011)
22. S. Capozziello, *Int. J. Mod. Phys. D* **11**, 483 (2002)
23. S.M. Carroll, V. Duvvuri, M. Trodden, M.S. Turner, *Phys. Rev. D* **70**, 043528 (2004)
24. S. Nojiri, S.D. Odintsov, *Phys. Rev. D* **68**, 123512 (2003)
25. S. Nojiri, S.D. Odintsov, *Phys. Lett. B* **657**, 238 (2007)
26. S. Nojiri, S.D. Odintsov, *Phys. Rev. D* **77**, 026007 (2008)
27. A.A. Starobinsky, *Phys. Lett. B* **99**, 24 (1980)
28. T.P. Sotiriou, V. Faraoni, *Rev. Mod. Phys.* **82**, 451 (2010)
29. R. Ferraro, F. Fiorini, *Phys. Rev. D* **75**, 084031 (2007)
30. R. Ferraro, F. Fiorini, *Phys. Rev. D* **78**, 124019 (2008)
31. G.R. Bengochea, R. Ferraro, *Phys. Rev. D* **79**, 124019 (2009)
32. M.V. de S Silva, M.E. Rodrigues, *Eur. Phys. C* **78**, 638 (2018)
33. T.P. Sotiriou, V. Faraoni, *Rev. Mod. Phys.* **82**, 451 (2010)
34. J.D. Barrow, S. Cotsakis, *Phys. Lett. B* **214**, 515 (1988)
35. K.-i Maeda, *Phys. Rev. D* **39**, 3159 (1989)
36. D.N. Vollick, *Phys. Rev. D* **68**, 063510 (2003)
37. G. Allemandi, A. Borowiec, M. Francaviglia, *Phys. Rev. D* **70**, 043524 (2004)

38. G. Allemandi, A. Borowiec, M. Francaviglia, Phys. Rev. D **70**, 103503 (2004)
39. G. Allemandi, A. Borowiec, M. Francaviglia, S.D. Odintsov, Phys. Rev. D **72**, 063505 (2005)
40. J.D. Barrow, A.C. Ottewill, J. Phys. A **16**, 2757 (1983)
41. S. Capozziello, V.F. Cardone, M. Francaviglia, Gen. Relativ. Gravit. **38**, 711 (2006)
42. M. Amarzguoui et al., Astron. Astrophys. **454**, 707 (2006)
43. T.P. Sotiriou, Class. Quantum Gravity **23**, 1253 (2006)
44. S. Fay, R. Tavakol, S. Tsujikawa, Phys. Rev. D **75**, 063509 (2007)
45. A. Borowiec, W. Godłowski, M. Szydlowski, Phys. Rev. D **74**, 043502 (2006)
46. A.V. Astashenok, S. Capozziello, S.D. Odintsov, Phys. Rev. D **89**, 103509 (2014)
47. A.V. Astashenok et al., JCAP **12**, 040 (2013)
48. A.V. Astashenok et al., Class. Quantum Gravity **34**, 205008 (2017)
49. T. Chiba, Phys. Lett. B **575**, 1 (2003)
50. A.L. Erickcek, T.L. Smith, M. Kamionkowski, Phys. Rev. D **74**, 121501(R) (2006)
51. I. Navarro, K.V. Acoleyen, J. Cosmol. Astropart. Phys. **JCAP02**, 022 (2007)
52. G.J. Olmo, Phys. Rev. Lett. **95**, 261102 (2005)
53. G.J. Olmo, Phys. Rev. D **72**, 083505 (2005)
54. G.J. Olmo, Phys. Rev. D **75**, 023511 (2007)
55. L. Amendola, D. Polarski, S. Tsujikawa, Phys. Rev. Lett. **98**, 131302 (2007)
56. S. Nojiri, S.D. Odintsov, Int. J. Geom. Methods. Mod. Phys. **04**, 114–45 (2007)
57. S. Nojiri, S.D. Odintsov, Phys. Rev. D **74**, 086005 (2006)
58. O. Mena, J. Santiago, J. Weller, Phys. Rev. Lett. **96**, 041103 (2006)
59. S. Fay, S. Nesseris, L. Perivolaropoulos, Phys. Rev. D **76**, 063504 (2007)
60. J.D. Barrow, T. Clifton, Phys. Rev. D **73**, 103520 (2006)
61. L.P. Chimento, Phys. Rev. D **81**, 043525 (2010)
62. M. Jamil, E.N. Saridakis, M.R. Setare, Phys. Rev. D **81**, 023007 (2010)
63. S.Z.W. Lip, Phys. Rev. D **83**, 023528 (2011)
64. F.E.M. Costa, J.S. Alcaniz, D. Jain, Phys. Rev. D **85**, 107302 (2012)
65. A.A. Starobinsky, JETP Lett. **30**, 682–685 (1979)
66. A.H. Guth, Phys. Rev. D **23**, 347 (1981)
67. A.D. Linde, *Inflation and Quantum Cosmology* (Academic, New York, 1990)
68. T. Banks, W. Fischler (2001). [arXiv:hep-th/0102077](https://arxiv.org/abs/hep-th/0102077)
69. T. Banks, W. Fischler (2001). [arXiv:hep-th/0111142](https://arxiv.org/abs/hep-th/0111142)
70. V. Sahni, A.A. Starobinsky, Int. J. Mod. Phys. D **9**, 373 (2000)
71. A.P. Billyard, A.A. Coley, Phys. Rev. D **61**, 083503 (2000)
72. B. Gumjudpai et al., JCAP **0506**, 007 (2005)
73. W. Zimdahl, D. Pavon, Class. Quantum Gravity **24**, 5461 (2007)
74. L. Amendola, G.C. Campos, R. Rosenfeld, Phys. Rev. D **75**, 083506 (2007)
75. H.M. Sadjadi, M. Honardoost, Phys. Lett. B **647**, 231 (2007)
76. M. Quartin et al., JCAP **0805**, 007 (2008)
77. J. Valiviita, R. Maartens, E. Majerotto, Mon. Not. R. Astron. Soc. **402**, 2355 (2010)
78. L.P. Chimento, Phys. Rev. D **81**, 043525 (2010)
79. M. Thorsrud, D.F. Mota, S. Hervik, JHEP **1210**, 066 (2012)
80. S. Pan, A. Mukherjee, N. Banerjee, Mon. Not. R. Astron. Soc. **477**, 1189 (2018)
81. S. Kumar, R.C. Nunes, Phys. Rev. D **96**(10), 103511 (2017)
82. E. Di Valentino, A. Melchiorri, O. Mena, Phys. Rev. D **96**, 043503 (2017)
83. W. Yang, S. Pan, A. Paliathanasis, Mon. Not. R. Astron. Soc. **482**(1), 1007–1016 (2019)
84. G. Cognola, E. Elizalde, S. Nojiri, S.D. Odintsov, S. Zerbini, Phys. Rev. D **73**, 084007 (2006)
85. S.S. da Costa et al., Class. Quantum Gravity **35**, 075013 (2018)
86. M. Benetti et al., Int. J. Mod. Phys. D **27**, 1850084 (2018)
87. M. De Laurentis, A.J. Lopez-Revelles, Int. J. Geom. Methods Mod. Phys. **11**, 1450082 (2014)
88. S.D. Odintsov et al., Nucl. Phys. B **938**, 935–956 (2018)
89. S.D. Odintsov et al., Class. Quantum Gravity **38**, 075009 (2021)
90. W. Hu, I. Sawicki, Phys. Rev. D **76**, 064004 (2007)
91. K. Bamba et al., Class. Quantum Gravity **30**, 015008 (2013)
92. S.D. Odintsov et al., Phys. Dark Universe **29**, 100563 (2020)
93. S.D. Odintsov, V.K. Oikonomou, Ann. Phys. **418**, 168186 (2020)
94. S.D. Odintsov, V.K. Oikonomou, Phys. Rev. D **101**, 044009 (2020)
95. V. Sahni et al., J. Exp. Theor. Phys. Lett. **77**, 201 (2003)
96. B.C. Paul, A. Majumdar, Class. Quantum Gravity **32**, 115001 (2015)
97. T. Clemson, K. Koyama, G.B. Zhao, R. Maartens, J. Valiviita, Phys. Rev. D **85**, 043007 (2012)
98. J. Valiviita, E. Majerotto, R. Maartens, JCAP **0807**, 020 (2008)
99. B.P. Abbott et al., Multi-messenger observations of a binary neutron star merger. Astrophys. J. **848**(2), L12 (2017)
100. W. Yang, S. Pan, D.F. Mota, Phys. Rev. D **96**(12), 123508 (2017)
101. W. Yang, S. Pan, J.D. Barrow, Phys. Rev. D **97**(4), 043529 (2018)
102. N. Aghanim et al. (Planck Collaboration) (2018) A & A **641**, A6 (2020)
103. B.C. Paul et al., Class. Quantum Gravity **39**, 065006 (2022)
104. S.D. Odintsov et al., Phys. Rev. D **102**, 104042 (2020)
105. J.C. Hwang, H. Noh, Phys. Rev. D **71**, 063536 (2005)
106. V.K. Oikonomou, F.P. Fronimos, [arXiv:2007.11915](https://arxiv.org/abs/2007.11915)
107. S.D. Odintsov, V.K. Oikonomou, Phys. Lett. B **805**, 135437 (2005)
108. N. Suzuki et al., Astrophys. J. **746**, 85 (2012)
109. R. Lazkoz, S. Nesseris, L. Perivolaropoulos, JCAP **0511**, 010 (2005)
110. A. Ali, A.S. Majumdar, JCAP **01**, 054 (2017)
111. T. Padmanabhan, Phys. Rep. **380**, 235 (2003)
112. E. Copeland, M. Sami, S. Tsujikawa, IJMPD **15**(11), 1752–1935 (2006)
113. S. Nojiri, S.D. Odintsov, IJGMMP **04**(01), 115–145 (2007)
114. H. Jassal, J. Bagla, T. Padmanabhan, Phys. Rev. D **72**, 103503 (2005)
115. S. Nesseris, L. Perivolaropoulos, Phys. Rev. D **73**, 103511 (2006)
116. S. Nesseris, L. Perivolaropoulos, JCAP **01**, 018 (2007)
117. B. Zwiebach, in *Anomalies, Geometry and Topology, Proceedings of the symposium, Argonne, Illinois*, ed. by W. A. Bardeen, A. White. (World Scientific Publication 1985); B. Zwiebach, Phys. Lett. B **156**, 315 (1985)
118. G. 't. Hooft, M. J. G. Veltman, Ann. Inst. Henri Poincaré **20**, 69 (1974)
119. G. 't. Hooft, Functional and probabilistic methods in quantum field theory, in *Proceedings of the XII Winter School on Theoretical Physics, Karpacz, Poland (1975)*, ed. by B. Jancewicz (Wydawnictwa Uniwersytetu Wrocławskiego, Wrocław, 1976)
120. B. Zumino, Phys. Rep. **137**, 109 (1986)
121. D.G. Boulware, S. Deser, Phys. Rev. Lett. **55**, 2656 (1985)
122. D.G. Boulware, S. Deser, Phys. Lett. B **175**, 409 (1986)
123. M. Gasperini et al., Nucl. Phys. B **494**, 315 (1997)
124. D. Lovelock, J. Math. Phys. **12**, 498 (1971)
125. I. Antoniadis et al., Nucl. Phys. B **415**, 497 (1994)
126. P. Kanti, J. Rizos, K. Tamva, Phys. Rev. D **59**, 083512 (1999)
127. S. Nojiri, S.D. Odintsov, M. Sasaki, Phys. Rev. D **71**, 123509 (2005)
128. G. Cognola et al., Phys. Rev. D **75**, 086002 (2007)
129. K. Bamba et al., JCAP **04**, 001 (2015)
130. B.C. Paul, S. Mukherjee, Phys. Rev. D **42**, 2595 (1990)
131. B.C. Paul, S. Ghose, Gen. Relativ. Gravit. **42**, 795–812 (2010)
132. B.C. Paul, S.D. Maharaj, A. Beesham, IJMPD **31**(06), 2250045 (2022)